Toward in Situ Biochemistry: Combining Chemical Kinetics Approaches with Biomolecular Imaging in Living Cells

Thomas F. Chancellor Jr.,[†] Robert J. Russell,[†] Vineet Dravid,[‡] and Tanmay P. Lele*,[†]

Department of Chemical Engineering, University of Florida, Museum Road, Bldg. 723, Gainesville, Florida 32611-6005, and COMSOL, Inc., 1 New England Executive Park, Suite 350, Burlington, Massachusetts 01803

Our knowledge of protein−protein interactions comes primarily from experimentation with reconstituted proteins in dilute solutions. However, dilute solutions are poor approximations of the intracellular microenvironment, which contains exquisite and dynamic structure that is impossible to recreate inside test tubes. New approaches are needed that will allow the in situ characterization of protein−protein interactions inside living, intact cells. In this paper, we discuss recent efforts to measure the kinetics of protein binding within complexes inside living cells. While the experimental effort in these studies requires the confluence of techniques ranging from molecular imaging to cell and molecular biology, the experimental design and analysis requires a strong background in chemical kinetics and transport phenomena. Thus, we argue that chemical engineers can play a central role in furthering in situ approaches to cellular analysis. Such efforts may aid significantly in advancing quantitative knowledge of cellular signaling and physiology.

Introduction

The majority of proteins inside living cells function by transiently binding to other species to form multimolecular complexes (*1*). These complexes are labile and are in a state of constant, dynamic assembly and disassembly. Unfortunately, current knowledge of protein−protein binding comes from experiments that involve the destruction of cells, the purification of the macromolecule of interest, and subsequent analysis by biochemical methods. Disrupting the cell and centrifuging its contents inevitably destroys supramolecular complexes. In addition, the assembly of such complexes is spatially and temporally regulated inside living cells. As a result, information gathered from in vitro studies are poor approximations of in situ behavior (*2*). New approaches are therefore needed that would allow the unambiguous measurement of protein function inside living cells.

In the past decade, remarkable strides have been made in visualizing macromolecules of interest inside living cells. These advances have been enabled in part due to the facile "marking" of the target macromolecule with a fluorescent tag. The fluorescent tag commonly used is the green fluorescent protein (GFP) (*3*), a protein isolated from the jellyfish *Aequorea victoria*. The GFP gene can be fused to any gene of interest using standard molecular biology techniques, and the resulting chimeric fusion protein can be expressed inside mammalian cells. The remarkable finding is that with few exceptions, GFP retains its fluorescence in the chimeric fusion protein, and the target macromolecule retains its function. As a result, it becomes possible to visualize any protein of interest inside living cells using videofluorescence microscopy (as opposed to more traditional immunolabeling of proteins that cannot be done inside a live cell).

* To whom correspondence should be addressed. Ph: 352-392-0317. Fax: 352-392-9513. E-mail: tlele@che.ufl.edu.

[†] University of Florida.

[‡] COMSOL, Inc.

Given that protein function inside cells involves transient binding interactions with their partners, the measurement of rate constants that characterize these interactions is of primary importance. In the perfect scenario, quantitative methods that can measure mechanisms and rates of (1) macromolecular transport, (2) macromolecular binding and dissociation, and (3) enzymatic activity inside the living cellular microenvironment are needed. Knowledge of these parameters and comparison with similar parameters measured in vitro may allow increased and unique insight into protein behavior. Additionally, these parameters would also represent a crucial (and as yet missing) input into systems-biology models of intracellular signaling.

The fluorescence recovery after photo bleaching (FRAP) technique has been used over the past three decades to measure the mobility of macromolecules. Originally developed for measuring diffusion coefficients of macromolecules in solution (*4*), this technique has been applied to a variety of problems including diffusion of liposaccharides in bacterial membranes (*5*), probe diffusion in gels (*6*) and tissues (*7*), macromolecular diffusion inside living cells (*8*), transport in the endoplasmic reticulum and Golgi (*9*), and nucleocytoplasmic transport (*10*). In FRAP, a specific area of interest is exposed to a small spot inside the cell with a short pulse of high-intensity irradiation at the excitation wavelength of the fluorophore (Figure 1A). This exposure irreversibly photobleaches the fluorophore without disrupting the function of the target molecule (*11*), so that the target molecule while physically present is optically invisible (such laser irradiation can have potential negative effects such as phototoxicity (*12*) and photodamage (*13*); it is very important to calibrate the laser intensity and exposure time before interpreting experiments). Fluorescence recovery occurs in the photobleached spot owing to diffusion of fluorescently tagged target molecules from outside into the spot. Recording the time-dependent increase in the fluorescence intensity in the bleached spot (Figures 2and 3) and combining this measurement with

10.1021/bp070110a CCC: $37.00
Published on Web 09/26/2007

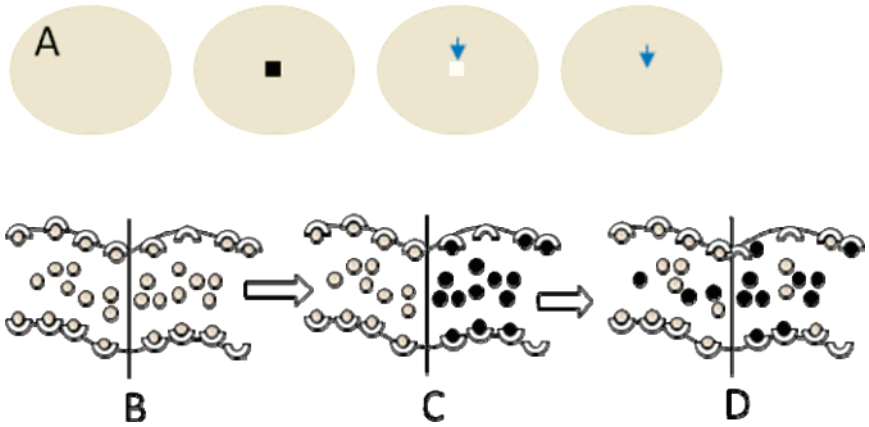

Figure 1. Schematic of the FRAP experiment and molecular model of recovery. (A) Fluorescent molecules in the nucleus are bleached at a predefined spot (black square) using a high-energy laser pulse. Time-dependent recovery occurs in the square due to interplay between molecular transport and binding (denoted by arrows in subsequent frames). (B) Before photobleaching, the bound molecules are in equilibrium with the free molecules. (C) After photobleaching, diffusion of fluorescent molecules (gray circles) occurs into the spot, followed by (D) subsequent exchange with photobleached bound molecules (black circles).

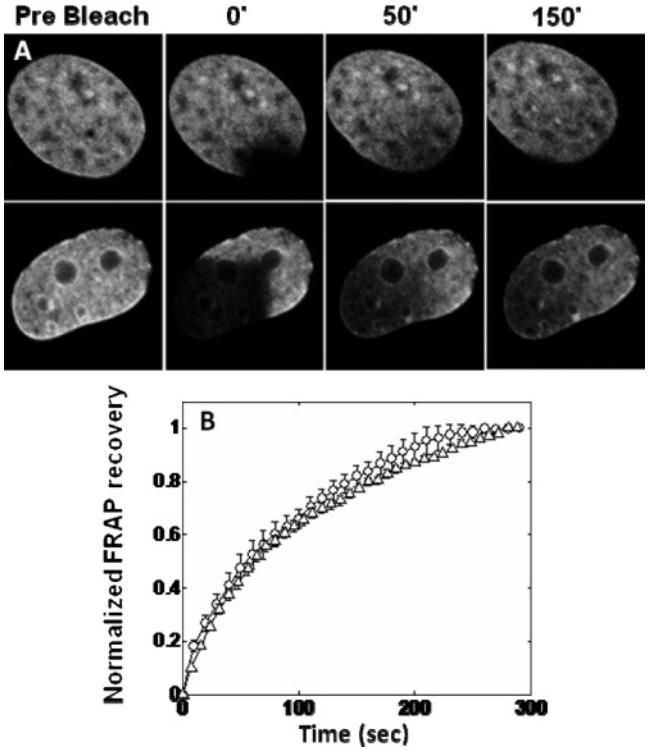

Figure 2. FRAP recovery of GFP-Histone H1 is insensitive to spot size. (A) Fluorescence confocal microscopic images recorded during FRAP analysis of NIH 3T3 cells expressing GFP-histone H1 in which small (top; 16 μm^2) or large (bottom; 125 μm^2) areas of the nucleus were photobleached (bar, 4 μm). (B) Recovery curve corresponding to the data in panel A normalized for differences in total fluorescence recovery, such that the fluorescence intensity in the bleached spot is zero immediately after laser exposure and 1 after complete recovery. Note that this time-dependent recovery is similar for the small (○) and large (△) spot sizes. (Modified with permission from ref 29; copyright 2006 by Wiley-Liss, Inc.)

mathematical models of diffusion will yield the diffusion coefficient of the chimeric protein.

If a considerable fraction of target molecules in the bleached spot are reversibly bound (either to structures or binding partners), then the recovery curve can yield the binding and dissociation rate constants describing protein−protein interactions inside a living cell (Figure 1B). While this tantalizing prospect was anticipated more than a decade ago (*14*, *15*), there has been a recent explosion of activity in this area. In particular, there has been considerable interest in understanding binding interactions of chromatin with proteins inside the living nucleus. These include using FRAP to quantify the kinetics of nuclear receptor-chromatin and transcription factor-chromatin binding (*16*−*27*), histone-chromatin binding (*28*−*32*), protein-nuclear matrix interactions (*33*, *34*), the assembly of transcriptional machinery (*35*), and the assembly of nuclear pore complexes in vivo (*36*). More recently, similar methods have been applied to study the assembly of cell-substrate adhesions (*37*−*40*). With such studies has come the recognition that the extraction of molecular binding kinetics from FRAP experiments requires the correct identification of the rate-limiting step during fluorescence recovery. The problem is essentially of modeling the coupling between transport and reaction, which has long been the special expertise of chemical engineers. In this paper, we will discuss mathematical models used for interpreting these experiments, the experimental design, and resulting insight into cellular function in the context of two problems: (1) cell-substrate adhesion and (2) DNA−protein interactions.

Linearity in FRAP models

Protein residence times in supramolecular complexes are typically smaller that the overall time scales of supramolecular complex assembly and disassembly. Over the time scale of the FRAP experiment, the structure can be assumed to be at local equilibrium (*28*). In FRAP, only the fluorescent tag is disrupted; the target molecule remains untouched. The total concentration of the target species always remains constant throughout the FRAP experiment, and only the fluorescence intensity of the marker changes. As a result, the mathematical model for the recovery process should be formulated in a manner that ensures that the concentrations of both the fluorescent and photobleached molecules at any time during the recovery process add up to the initial steady-state concentration of fluorescent species.

In general, the above constraint will lead to linear kinetic terms in the model equations. To see this, consider a fluorescent species disappearing with an arbitrary nonlinear reaction rate $r(C_0)$ where C_0 is the equilibrium concentration before the photobleaching process. After photobleaching, two species are created, C_F (fluorescent) and C_P (photobleached). As these two species are absolutely similar except that C_P is optically invisible, the reaction rate at which C_F disappears in the photobleached spot is a fraction of the original reaction rate and is given by $C_F/(C_F + C_P)\ r(C_{0)} = C_F/C_0\ r(C_0)$. This is linear in C_F. The corresponding rate of disappearance of C_P is $C_P/C_0\ r(C_0)$. The

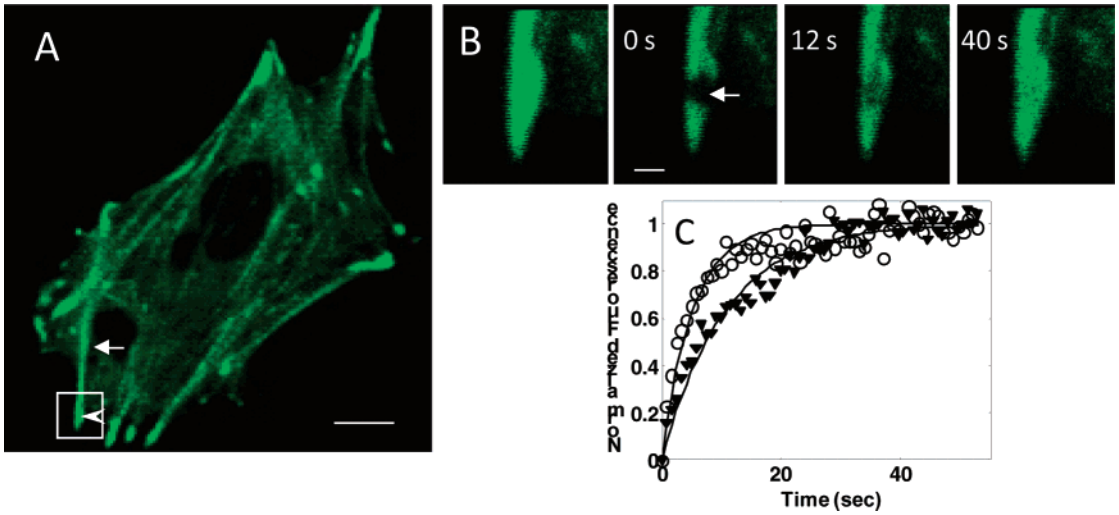

Figure 3. Tension accelerates recovery of a focal adhesion protein. (A) Confocal fluorescence micrograph of a single capillary endothelial cell expressing zyxin. Zyxin decorates stress fibers (arrow) that terminate into adhesions (arrowhead). Scale bar is 10 μm. (B) A representative FRAP experiment with GFP-zyxin inside a single focal adhesion (inset), in which a ~0.5 μm^2 area was bleached (white arrow) and subsequent time-dependent fluorescence recovery recorded by capturing confocal fluorescence images (bar = 1 μm). (C) Dependence of zyxin exchange dynamics on intracellular tension. The curves show time-dependent recovery of fluorescence intensity for GFP-zyxin in control cells (○) versus cells in which tension was dissipated by treating cells with Y27632 (▼); solid lines are curve-fits to $1 - e^{-k_{OFF}t}$ using the method of least-squares to estimate k_{OFF}. (Modified with permission from ref 37, copyright 2006 by Wiley-Liss, Inc.)

two rates will add up to the equilibrium reaction rate of $r(C_0)$, which is to be expected since the net reaction rate is unchanged during the experiment. In general, the kinetic terms in FRAP models will be linear (assuming the structure is at steady state before the bleach).

FRAP Model for Macromolecular Binding to Nuclear Structure

There is considerable interest in measuring the rate constants describing binding and dissociation of nuclear proteins to chromatin. Many nuclear proteins have a diffuse staining inside the nucleus (i.e., no localization to specific binding sites) where it is not possible to distinguish between bound and free concentrations. In addition, binding sites are frequently distributed uniformly throughout the nucleus. As a result, FRAP experiments with nuclear proteins that have diffuse staining are typically modeled as having a uniform distribution of binding sites throughout the domain. This is analogous to models of supported catalysts where free molecules diffuse in the interstices of the catalyst, while binding to random oriented catalytic scaffolds. Denoting free nuclear molecules by A and available binding sites by S, then the binding reaction can be written as

$$A + S \leftrightarrow AS \tag{1}$$

where AS denotes bound molecules of A. Without making the distinction between bleached or fluorescent species, the governing equations for protein transport on the domain Ω (e.g,. the entire nucleus) are

$$\frac{\partial C}{\partial t} = D\nabla^2 C - k_{ON} C S(\hat{C}) + k_{OFF}\hat{C} \tag{2}$$

$$\frac{\partial \hat{C}}{\partial t} = k_{ON} C S(\hat{C}) - k_{OFF}\hat{C} \tag{3}$$

along with $\nabla C \cdot \mathbf{n} = \mathbf{0}$ on the boundary $\partial\Omega$ (i.e., on the nuclear boundary), which signifies that there is no flux of molecules outside the domain on the time scale of the FRAP experiment. The bound species is assumed to not diffuse, although this may not be true for some complexes (such as the ribonucleoprotein complex (*41*)). C is the concentration of free species, $\hat{C}$ is the concentration of bound species. k_{ON} and k_{OFF} are the rate constants for binding and dissociation, respectively. The function $S(\hat{C})$ is the fractional availability of binding sites and will in general depend nonlinearly on $\hat{C}$. One study assumed $S(\hat{C}) = 1 - \hat{C}/\tilde{C}_0$, where $\tilde{C}_0$ is the theoretical concentration of bound proteins if all binding sites were occupied (*28*). At steady state,

$$C = C_0; \quad \hat{C}_0 = \frac{k_{ON} C_0 \tilde{C}_0}{k_{ON} C_0 + k_{OFF}\tilde{C}_0} = \frac{C_0 \tilde{C}_0}{C_0 + K\tilde{C}_0} \tag{4}$$

where C_0 and $\hat{C}_0$ are the concentrations of the free and equilibrated bound protein at steady state and $K = k_{OFF}/k_{ON}$ is the equilibrium constant. Equation 4 can be rearranged to yield

$$\frac{\hat{C}_0}{\tilde{C}_0} = \frac{\gamma}{\gamma + K}; \quad \frac{\hat{C}_0}{C_0} = \frac{1}{\gamma + K} \tag{5}$$

where $\gamma \equiv C_0/\tilde{C}_0$. Let the concentration of photobleached free species be C_P and of fluorescent free species be C_F; similarly that of the bound species be $\hat{C}_P$ and $\hat{C}_F$. $C_P + C_F = C_0$ and $\hat{C}_P + \hat{C}_F = \hat{C}_0$ are valid throughout the domain, i.e., no gradients exist in the total concentration. The equations describing the recovery of *fluorescent* proteins in the photobleached spot are

$$\frac{\partial C_F}{\partial t} = D\nabla^2 C_F - k_{ON} C_F\left(1 - \frac{\hat{C}_0}{\tilde{C}_0}\right) + k_{OFF}\hat{C}_F \tag{6}$$

$$\frac{\partial \hat{C}_F}{\partial t} = k_{ON} C_F\left(1 - \frac{\hat{C}_0}{\tilde{C}_0}\right) - k_{OFF}\hat{C}_F \tag{7}$$

As the bound species has equilibrated with the free species before being photobleached, the number of available binding sites is a constant as embodied by the $(1 - \hat{C}_0/\hat{C}_0)$ term. Equations 6 and 7 are uncoupled from equations describing the photobleached concentration (the boundary conditions are uncoupled as well) and are linear; the bleached and fluorescent species concentrations can be solved for independently.

The time scale of recovery, τ_R, will depend on the interplay between binding, dissociation, and diffusion. The situation where

k_{ON} is vanishingly small (i.e., $K \gg 1$) is ignored, because then $\hat{C}_0 \rightarrow 0$ (see eq 5). Similarly, the case where $\tilde{C}_0 \ll C_0$ (i.e., $\gamma \gg 1$) is ignored, because the contribution to the recovery curve by the bound species is negligible. As a result, cases where $\gamma + K \gg 1$ are ignored in the analysis.

The photobleached spot is assumed to be circular with a radius αR where R is the radius of the entire (circular) domain. We define the following dimensionless variables: $\xi = r/\alpha R$, $c_F = C_F/C_0$, $\tau_D \equiv (\alpha R)^2/D$, and $\hat{c}_F = \hat{C}_F/\hat{C}_0$. The equations become

$$\frac{\partial c_F}{\partial \tau} = \nabla^2 c_F - \frac{Da}{\gamma + K}(c_F - \hat{c}_F) \tag{8}$$

$$\frac{\partial \hat{c}_F}{\partial \tau} = Da(c_F - \hat{c}_F) \tag{9}$$

where ∇^2 is the cylindrical Laplacian operator. $Da \equiv k_{OFF}(\alpha R)^2/D$ is the Damköhler number and is the ratio of the characteristic time scale of diffusion to that of binding.

Two limiting cases for recovery are possible. If $Da/\gamma + K \gg 1$, over the time that $\nabla^2 c \sim 1$, $c - c_F \sim \gamma + K/Da$. Thus, $\partial c/\partial \tau \approx \partial \hat{c}/\partial \tau$, and combining eqs 8 and 9

$$\left(1 + \frac{1}{\gamma + K}\right)\frac{\partial c_F}{\partial \tau} = \nabla^2 c_F \tag{10}$$

From eq 10, the time scale for recovery τ_R is

$$\tau_R = \left(\frac{1}{\gamma + K} + 1\right)\tau_D = \left(\frac{1}{\gamma + K} + 1\right)\frac{\alpha^2 R^2}{D} \tag{11}$$

If $Da/\gamma + K \ll 1$, there are two time scales involved: τ_D over which $\partial c_F/\partial \tau = \nabla^2 c_F - Da/\gamma + K\,(c_F - \hat{c}_F) \sim \nabla^2 c_F$, and τ_{OFF} over which $c_F \sim$ constant and $1/Da\ \partial \hat{c}_F/\partial \tau = \partial \hat{c}_F/k_{OFF}\partial t = c_F - \hat{c}_F =$ constant $- \hat{c}_F$. Thus

$$\tau_R = \tau_{OFF} = \frac{1}{k_{OFF}} \tag{12}$$

Application of FRAP to Characterizing Macromolecular Interactions inside Living Cells

The mathematical model above and the scaling analysis suggest simple experiments to determine the rate-limiting step in experiments. We now discuss two recently published experimental studies (*29*, *37*) to measure rate constants of macromolecular binding inside living cells.

Histone H1−Chromatin Interaction

The packaging of ~2 m of DNA into the nucleus of human cells is enabled by the nucleosome, which is formed by the wrapping of DNA around a nucleosomal core consisting of an octamer complex with two molecules each of histones H2A, H2B, H3, and H4 (*42*, *43*). This forms a chromatin structure that appears as "beads on a string" when viewed in an electron microscope (*44*). Histone H1 binds to 23 base pairs of DNA that extend out from this nucleosomal core (*45*). The binding of histone H1 to chromatin allows further folding of nucleosomal strings into more condensed chromatin structures. This folding causes transcriptional repression, and there is evidence to suggest that the dissociation of histone H1 from chromatin could lead to activation of gene transcription (*46*). Binding of histone H1 to DNA has been characterized in vitro (*47*); however, the relevance of these results for its binding to DNA within intact chromatin remains unclear.

GFP-histone H1.1 is uniformly distributed in the nucleus without any clear concentration at clusters, as is evident from confocal fluorescence images of living nuclei (Figure 2). Other histones are also found to have a similar nuclear distribution, with no visible accumulation at binding clusters inside nuclei (*31*). This is probably due to the fact that the binding sites for histones (chromatin) are distributed uniformly throughout the nucleus. In addition, histone transport between the nucleus to the cytoplasm is negligible over FRAP time scales, suggesting the no-flux boundary condition.

Equation 11 suggests that if diffusion was rate-limiting, the recovery time during FRAP would increase quadratically with the spot size. When FRAP experiments with varying spot sizes in living NIH3T3 cells expressing EGFP-histone H1 were carried out (*29*), the recovery time was insensitive to the size of the spot (Figure 2). Diffusion is therefore not rate-limiting; this is supported by studies with a mutant GFP histone H1.1 that cannot bind to chromatin and was found to have very high diffusion coefficient (*48*, *49*). Thus, eq 12 suggests that the observed recovery for EGFP-histone H1 is determined by its dissociation rate constant. On fitting the normalized recovery curve to $1 - e^{-k_{OFF}t}$ yields a dissociation rate constant of 0.0131 /s for GFP histone H1.1 (*29*) inside living nuclei.

The dissociation of linker histones from chromatin is regulated to activate gene transcription (*46*). Serine phosphorylation of Histone H1 can regulate gene transcription in *Tetrahymena*. Interestingly, FRAP experiments suggest that the phosphorylation state of histone H1.1 controls its dissociation rate from chromatin, suggesting that the regulation of kinetics may be central to histone H1 function (*50*). Additionally, histone binding to HP1 during heterochromatin formation (*51*) could play a central role in stabilizing condensed chromatin structures. If all of these interactions are biologically significant, we might expect local alterations in histone H1 binding and unbinding rates that could, with appropriate biological manipulations, be probed with the methods discussed here.

The dissociation rate constant reported above is an effective rate constant that arises from multiple transient interactions between histone H1.1 and its binding partners. A central challenge for the future is the development of a rational approach that allows the inference of the kinetics of pairwise interactions from these "effective" kinetic measurements. One possibility is to combine FRAP with RNAi to eliminate binding partners or mutagenesis to interfere with individual binding interactions. This would help quantify the effect of individual interactions systematically on the effective dissociation rate constants by inputting data into an appropriate microscopic kinetic model. If successful, such an approach would yield invaluable information on how interactions between specific protein pairs are regulated inside living cells.

Separately, binding interactions between histone H1.1 and proteins such as the barrier-to-autointegration factor (BAF) have been demonstrated in vitro (*52*); however, the strength of this binding in situ is unknown. The above approach of measuring pairwise binding interactions may also serve as a quantitative tool for the systematic discovery of binding interactions (and their kinetics) in situ. This is important given that the number of interactions identified for proteins in vitro frequently ranges in the hundreds, whereas pure steric hindrances dictate that a given molecule may bind to only a few (four or five) other species simultaneously.

Protein−Protein Interactions in Cell-Substrate Adhesion

Anchorage-dependent cells attach to solid substrates at discrete sites called focal adhesions. Focal adhesions are formed when transmembrane receptors called integrins ligate to extracellular matrix (ECM) molecules such as fibronectin. Ligation and clustering of integrins results in a cascade of events that includes the recruitment of a large number of proteins including molecules that couple integrins to the cytoskeleton (e.g., α-actinin, talin), kinases and phosphatases that act on substrates in the adhesion complex (e.g., focal adhesion kinase), and adaptor molecules that allows multiple substrates to "dock" in adhesions through binding interactions (e.g., paxillin) (*53*). Mechanical forces generated in the actin cytoskeleton are transmitted through integrins to the ECM. Thus, the focal adhesion provides a path for mechanical force transfer from the inside of the cell onto the underlying substrate. This forms the basis for cell spreading, cell shape, and cell motility.

Focal adhesion assembly is regulated by tensile forces exerted by bundles of actin filaments called stress fibers that anchor into adhesions (Figure 3A). In stationary cells, cell-substrate adhesion size correlates directly with the level of traction force that is exerted on the substrate at these sites (*54*). When cytoskeletal tension is dissipated by inhibiting actomyosin contractility, adhesions disassemble (*53*). Additionally, mechanical force can directly cause adhesion assembly (*55*, *56*). This dependence of focal adhesion size, protein localization, and signaling on internal cytoskeletal prestress or external mechanical stress has led to the hypothesis that integrins act as mechanoreceptors (*57*, *58*) and that certain focal adhesion proteins function as mechanosensors by altering their conformation and/or binding kinetics in response to stress (*53*, *59*−*61*).

The mechanisms underlying force-dependent control of adhesion assembly remain poorly understood, although several models have been proposed. For example, force-dependent changes of conformation of proteins may expose cryptic binding sites and promote binding of molecules (*62*, *63*). Stretching detergent-insoluble cytoskeletons causes alterations in the cytoskeletal binding affinities of several cytoplasmic proteins, including the focal adhesion molecules paxillin and FAK (*64*).

Alternatively, mechanical forces could alter the binding kinetics of individual molecules that assemble into focal adhesions. A change in rate constants would alter the balance between binding and unbinding rates, giving rise to net assembly or disassembly of specific molecules from adhesions. To test this hypothesis, FRAP experiments were recently carried out in capillary endothelial cells expressing GFP-zyxin and GFP-vinculin, two proteins that localize to focal adhesions (Figure 3B). In these experiments, the photobleached spot was confined to the adhesion site and the bleaching was performed for very short times (less than 1 ms), leading to minimal bleaching of freely diffusing molecules. Also, owing to the small spot size (less than 0.5 μm^2), diffusion is expected to be rate-limiting (*37*), which was confirmed by carrying out independent experiments in the cytoplasm. Finally, the pool of diffusing molecules is in far excess of bound protein and hence is essentially unperturbed by the recovery process. Therefore, the assumption can be made that C_F is constant (*37*, *38*).

Under the specified imaging parameters, the FRAP experiment basically records the rate of exchange between bound molecules and free molecules and can be described by the differential equation $d\hat{C}_F/dt = k_{ON}SC_F - k_{OFF}\hat{C}_F$ with $\hat{C}_F(0) = \alpha\hat{C}_0$. Here, $\hat{C}_F$ is the concentration of bound fluorescent protein, C_F is the concentration of freely diffusing protein, S is the concentration of available binding sites, $\hat{C}_0 = k_{ON}SC_F/k_{OFF}$ is the prebleach concentration in the focal adhesion, and α denotes the fraction of fluorescent molecules that are not bleached in the photobleached spot. Assuming that S, the binding site concentration, is constant during the FRAP recovery, the solution to the above differential equation is $\hat{C}_F - \alpha\hat{C}_0/\hat{C}_0 - \alpha\hat{C}_0 = 1 - e^{-k_{OFF}t}$. Thus, time scales of fluorescence recovery in these experiments are again determined by k_{OFF}. The assumption that S is constant during FRAP recovery may be invalid if the adhesion complex is assembling or disassembling in motile cells; this situation has been modeled elsewhere (*38*).

Bound GFP-zyxin and GFP-vinculin have lifetimes much shorter than that of histone H1.1. While zyxin recovered with $k_{OFF} = 0.1 \pm 0.01$/s, vinculin exchanged with two time scales, corresponding to two subpopulations of bound molecules ($k_{OFF,1} = 0.06 \pm 0.01$/s and $k_{OFF,2} = 0.97 \pm 0.01$/s). Decreasing the force exerted on adhesions by myosin inhibition resulted in an increase in the exchange rate (Figure 3C) corresponding to an increase in k_{OFF} of zyxin (*37*), suggesting that force relaxation causes changes in the intra-adhesion binding interactions of zyxin. Surprisingly, similar experiments with vinculin revealed that the values of k_{OFF} corresponding to both of its two dynamically distinct subpopulations remained unchanged on force relaxation (*37*). Thus, the molecular binding kinetics of some but not all focal adhesion proteins are selectively sensitive to changes in cytoskeletal tension. Interestingly, the mechanically induced changes in dissociation rate constants measured for zyxin were sufficient to explain the overall unsteady disappearance of zyxin from adhesion sites in response to tension relaxation (*37*).

These findings are intriguing because there is evidence that zyxin acts as a mechanosensor owing to its redistribution from focal adhesions to stress fibers on application of mechanical force (*65*) and that vinculin binding to the cytoskeleton does not change on application of mechanical strain (*64*). A variety of other proteins including paxillin, RPTPα, focal adhesion kinase, Shp-2, and p130CAS have been shown to be involved in mechanosensation (*64*, *66*−*69*). The approach discussed in this paper may be potentially useful to better understand how these mechano-sensitive proteins orchestrate the mechanical and dynamic control of adhesion assembly.

Conclusion

FRAP is a promising technique that can be used to measure the rate constants of intermolecular interactions inside living cells. The method offers distinct advantages over in vitro biochemical methods of analysis that remove a protein from its native environment, destroying labile supramolecular complexes that it resides in. The in situ nature of the measurement means that FRAP analysis could dramatically improve our knowledge of protein function inside living cells. The experimental design and analysis of FRAP experiments requires knowledge of transport phenomena and reaction kinetics, which are traditional domains of chemical engineers. We anticipate that future refinements of such methods will allow the measurement of in situ pairwise binding interactions, the correlation of protein conformation changes with alterations in binding kinetics, and the enzymatic modulation of protein−protein interactions. Such quantitative measurements also represent an essential link between systems biology and the world of biological experimentation.

Acknowledgment

The authors wish to thank former mentors and colleagues in whose laboratories some of the work reviewed here was conducted, including Professors Donald Ingber and Jeffrey Nickerson.

References and Notes

(1) Alberts, B. The cell as a collection of protein machines: preparing the next generation of molecular biologists. *Cell* **1998**, *92* (3), 291−294.

(2) Luby-Phelps, K. Cytoarchitecture and physical properties of cytoplasm: volume, viscosity, diffusion, intracellular surface area. *Int. Rev. Cytol.* **2000**, *192*, 189−221.

(3) Tsien, R. Y. The green fluorescent protein. *Annu. Rev. Biochem.* **1998**, *67*, 509−544.

(4) Axelrod, D.; Koppel, D. E.; Schlessinger, J.; Elson, E.; Webb, W. W. Mobility measurement by analysis of fluorescence photobleaching recovery kinetics. *Biophys. J.* **1976**, *16* (9), 1055−1069.

(5) Schindler, M.; Osborn, M. J.; Koppel, D. E. Lateral diffusion of lipopolysaccharide in the outer membrane of *Salmonella typhimurium*. *Nature* **1980**, *285* (5762), 261−263.

(6) Cheng, Y.; Prud'homme, R.; Thomas, J. Diffusion of mesoscopic probes in acqueous polymer solutions using fluorescence recovery after photobleaching. *Macromolecules* **2002**, *35*, 8111−8121.

(7) Berk, D. A.; Yuan, F.; Leunig, M.; Jain, R. K. Fluorescence photobleaching with spatial Fourier analysis: measurement of diffusion in light-scattering media. *Biophys. J.* **1993**, *65* (6), 2428−2436.

(8) Luby-Phelps, K.; Castle, P. E.; Taylor, D. L.; Lanni, F. Hindered diffusion of inert tracer particles in the cytoplasm of mouse 3T3 cells. *Proc. Natl. Acad. Sci. U.S.A.* **1987**, *84* (14), 4910−4913.

(9) Lippincott-Schwartz, J.; Snapp, E.; Kenworthy, A. Studying protein dynamics in living cells. *Nat. Rev. Mol. Cell Biol.* **2001**, *2* (6), 444−456.

(10) Patterson, G. H.; Lippincott-Schwartz, J. A photoactivatable GFP for selective photolabeling of proteins and cells. *Science* **2002**, *297* (5588), 1873−1877.

(11) Phair, R. D.; Misteli, T. Kinetic modelling approaches to in vivo imaging. *Nat. Rev. Mol. Cell Biol.* **2001**, *2* (12), 898−907.

(12) Dobrucki, J. W.; Feret, D.; Noatynska, A. Scattering of exciting light by live cells in fluorescence confocal imaging−phototoxic effects and relevance for FRAP studies. *Biophys. J.* **2007**.

(13) O'Brien, E. M.; Gomes, D. A.; Sehgal, S.; Nathanson, M. H. Hormonal regulation of nuclear permeability. *J. Biol. Chem.* **2007**, *282* (6), 4210−4217.

(14) Kaufman, E. N.; Jain, R. K. Quantification, of transport and binding parameters using fluorescence recovery after photobleaching. Potential for in vivo applications. *Biophys. J.* **1990**, *58* (4), 873−885.

(15) Kaufman, E. N.; Jain, R. K. Measurement of mass transport and reaction parameters in bulk solution using photobleaching. Reaction limited binding regime. *Biophys. J.* **1991**, *60* (3), 596−610.

(16) Stenoien, D. L.; Nye, A. C.; Mancini, M. G.; Patel, K.; Dutertre, M.; O'Malley, B. W.; Smith, C. L.; Belmont, A. S.; Mancini, M. A. Ligand-mediated assembly and real-time cellular dynamics of estrogen receptor alpha-coactivator complexes in living cells. *Mol. Cell. Biol.* **2001**, *21* (13), 4404−4412.

(17) Ferrara, F. F.; Fazi, F.; Bianchini, A.; Padula, F.; Gelmetti, V.; Minucci, S.; Mancini, M.; Pelicci, P. G.; Lo Coco, F.; Nervi, C. Histone deacetylase-targeted treatment restores retinoic acid signaling and differentiation in acute myeloid leukemia. *Cancer Res.* **2001**, *61* (1), 2−7.

(18) Stenoien, D. L.; Patel, K.; Mancini, M. G.; Dutertre, M.; Smith, C. L.; O'Malley, B. W.; Mancini, M. A. FRAP reveals that mobility of oestrogen receptor-alpha is ligand- and proteasome-dependent. *Nat. Cell Biol.* **2001**, *3* (1), 15−23.

(19) Stenoien, D. L.; Mancini, M. G.; Patel, K.; Allegretto, E. A.; Smith, C. L.; Mancini, M. A. Subnuclear trafficking of estrogen receptor-alpha and steroid receptor coactivator-1. *Mol. Endocrinol.* **2000**, *14* (4), 518−534.

(20) Sharp, Z. D.; Mancini, M. G.; Hinojos, C. A.; Dai, F.; Berno, V.; Szafran, A. T.; Smith, K. P.; Lele, T. P.; Ingber, D. E.; Mancini, M. A. Estrogen-receptor-alpha exchange and chromatin dynamics are ligand- and domain-dependent. *J. Cell Sci.* **2006**, *119* (Pt 19), 4101−4116.

(21) Sprague, B. L.; Pego, R. L.; Stavreva, D. A.; McNally, J. G. Analysis of binding reactions by fluorescence recovery after photobleaching. *Biophys. J.* **2004**, *86* (6), 3473−3495.

(22) Sprague, B. L.; Mueller, F.; Pego, R. L.; Bungay, P. M.; Stavreva, D. A.; McNally, J. G. Analysis of binding at a single spatially localized cluster of binding sites by fluorescence recovery after photobleaching. *Biophys. J.* **2006**, *91* (4), 1169−1191.

(23) Laricchia-Robbio, L.; Tamura, T.; Karpova, T.; Sprague, B. L.; McNally, J. G.; Ozato, K. Partner-regulated interaction of IFN regulatory factor 8 with chromatin visualized in live macrophages. *Proc. Natl. Acad. Sci. U.S.A.* **2005**, *102* (40), 14368−14373.

(24) Sprague, B. L.; McNally, J. G. FRAP analysis of binding: proper and fitting. *Trends Cell Biol.* **2005**, *15* (2), 84−91.

(25) Karpova, T. S.; Chen, T. Y.; Sprague, B. L.; McNally, J. G. Dynamic interactions of a transcription factor with DNA are accelerated by a chromatin remodeller. *EMBO Rep.* **2004**, *5* (11), 1064−1070.

(26) Phair, R. D.; Scaffidi, P.; Elbi, C.; Vecerova, J.; Dey, A.; Ozato, K.; Brown, D. T.; Hager, G.; Bustin, M.; Misteli, T. Global nature of dynamic protein-chromatin interactions in vivo: three-dimensional genome scanning and dynamic interaction networks of chromatin proteins. *Mol. Cell. Biol.* **2004**, *24* (14), 6393−6402.

(27) Phair, R. D.; Gorski, S. A.; Misteli, T. Measurement of dynamic protein binding to chromatin in vivo, using photobleaching microscopy. *Methods Enzymol.* **2004**, *375*, 393−414.

(28) Lele, T. P.; Oh, P.; Nickerson, J. A.; Ingber, D. An improved mathematical model for determination of molecular kinetics in living cells with FRAP. *Mech. Chem. Biosyst.* **2004**, *1* (3), 181−190.

(29) Lele, T.; Wagner, S. R.; Nickerson, J. A.; Ingber, D. E. Methods for measuring rates of protein binding to insoluble scaffolds in living cells: histone H1-chromatin interactions. *J. Cell. Biochem.* **2006**, *99* (5), 1334−1342.

(30) McManus, K. J.; Biron, V. L.; Heit, R.; Underhill, D. A.; Hendzel, M. J. Dynamic changes in histone H3 lysine 9 methylations: identification of a mitosis-specific function for dynamic methylation in chromosome congression and segregation. *J. Biol. Chem.* **2006**, *281* (13), 8888−8897.

(31) Th'ng, J. P.; Sung, R.; Ye, M.; Hendzel, M. J. H1 family histones in the nucleus. Control of binding and localization by the C-terminal domain. *J. Biol. Chem.* **2005**, *280* (30), 27809−27814.

(32) Bhattacharya, D.; Mazumder, A.; Miriam, S. A.; Shivashankar, G. V. EGFP-tagged core and linker histones diffuse via distinct mechanisms within living cells. *Biophys. J.* **2006**, *91* (6), 2326−2336.

(33) Wagner, S.; Chiosea, S.; Ivshina, M.; Nickerson, J. A. In vitro FRAP reveals the ATP-dependent nuclear mobilization of the exon junction complex protein SRm160. *J. Cell Biol.* **2004**, *164* (6), 843−850.

(34) Wagner, S.; Chiosea, S.; Nickerson, J. A. The spatial targeting and nuclear matrix binding domains of SRm160. *Proc. Natl. Acad. Sci. U.S.A.* **2003**, *100* (6), 3269−3274.

(35) Dundr, M.; Hoffmann-Rohrer, U.; Hu, Q.; Grummt, I.; Rothblum, L. I.; Phair, R. D.; Misteli, T. A kinetic framework for a mammalian RNA polymerase in vivo. *Science* **2002**, *298* (5598), 1623−1626.

(36) Rabut, G.; Doye, V.; Ellenberg, J. Mapping the dynamic organization of the nuclear pore complex inside single living cells. *Nat. Cell Biol.* **2004**, *6* (11), 1114−1121.

(37) Lele, T. P.; Pendse, J.; Kumar, S.; Salanga, M.; Karavitis, J.; Ingber, D. E. Mechanical forces alter zyxin unbinding kinetics within focal adhesions of living cells. *J. Cell. Physiol.* **2006**, *207* (1), 187−194.

(38) Lele, T. P.; Ingber, D. E. A mathematical model to determine molecular kinetic rate constants under non-steady state conditions using fluorescence recovery after photobleaching (FRAP). *Biophys. Chem.* **2006**, *120* (1), 32−35.

(39) Lele, T.; Thodeti, C. K.; Ingber, D. E. Force meets chemistry: Analysis of mechanochemical conversion in focal adhesions using fluorescence recovery after photobleaching. *J. Cell. Biochem.* **2006**, *97* (6), 1175−1183.

(40) Lele, T.; Sero, J.; Matthews, B.; Kumar, S.; Montoya, M.; Polte, T.; Overby, D.; Ingber, D. E. Tools to study cell mechanics and mechanotransduction. *Methods Cell Biol.* **2007**, *83*, 441−472.

(41) Braga, J.; McNally, J. G.; Carmo-Fonseca, M. A reaction-diffusion model to study RNA motion by quantitative fluorescence recovery after photobleaching. *Biophys. J.* **2007**, *92* (8), 2694−2703.
(42) Richmond, T. J.; Finch, J. T.; Rushton, B.; Rhodes, D.; Klug, A. Structure of the nucleosome core particle at 7 A resolution. *Nature* **1984**, *311* (5986), 532−537.
(43) Luger, K.; Mader, A. W.; Richmond, R. K.; Sargent, D. F.; Richmond, T. J. Crystal structure of the nucleosome core particle at 2.8 Å resolution. *Nature* **1997**, *389* (6648), 251−260.
(44) Olins, A. L.; Olins, D. E. Spheroid chromatin units (v bodies). *Science* **1974**, *183* (122), 330−332.
(45) Travers, A. The location of the linker histone on the nucleosome. *Trends Biochem. Sci.* **1999**, *24* (1), 4−7.
(46) Zlatanova, J.; Caiafa, P.; Van Holde, K. Linker histone binding and displacement: versatile mechanism for transcriptional regulation. *FASEB J.* **2000**, *14* (12), 1697−1704.
(47) Mamoon, N. M.; Song, Y.; Wellman, S. E. Binding of histone H1 to DNA is described by an allosteric model. *Biopolymers* **2005**, *77* (1), 9−17.
(48) Hendzel, M. J.; Lever, M. A.; Crawford, E.; Th'ng, J. P. The C-terminal domain is the primary determinant of histone H1 binding to chromatin in vivo. *J. Biol. Chem.* **2004**, *279* (19), 20028−20034.
(49) Lever, M. A.; Th'ng, J. P.; Sun, X.; Hendzel, M. J. Rapid exchange of histone H1.1 on chromatin in living human cells. *Nature* **2000**, *408* (6814), 873−876.
(50) Dou, Y.; Bowen, J.; Liu, Y.; Gorovsky, M. A. Phosphorylation and an ATP-dependent process increase the dynamic exchange of H1 in chromatin. *J. Cell Biol.* **2002**, *158* (7), 1161−1170.
(51) Nielsen, A. L.; Oulad-Abdelghani, M.; Ortiz, J. A.; Remboutsika, E.; Chambon, P.; Losson, R. Heterochromatin formation in mammalian cells: interaction between histones and HP1 proteins. *Mol. Cell* **2001**, *7* (4), 729−739.
(52) Montes de Oca, R.; Lee, K. K.; Wilson, K. L. Binding of barrier-to-autointegration factor (BAF) to histone H3 and selected linker histones including H1.1. *J. Biol. Chem.* **2005**, *280* (51), 42252−42262.
(53) Bershadsky, A. D.; Balaban, N. Q.; Geiger, B. Adhesion-dependent cell mechanosensitivity. *Annu. Rev. Cell Dev. Biol.* **2003**, *19*, 677−695.
(54) Balaban, N. Q.; Schwarz, U. S.; Riveline, D.; Goichberg, P.; Tzur, G.; Sabanay, I.; Mahalu, D.; Safran, S.; Bershadsky, A.; Addadi, L.; Geiger, B. Force and focal adhesion assembly: a close relationship studied using elastic micropatterned substrates. *Nat. Cell Biol.* **2001**, *3* (5), 466−472.
(55) Riveline, D.; Zamir, E.; Balaban, N. Q.; Schwarz, U. S.; Ishizaki, T.; Narumiya, S.; Kam, Z.; Geiger, B.; Bershadsky, A. D. Focal contacts as mechanosensors: externally applied local mechanical force induces growth of focal contacts by an mDia1-dependent and ROCK-independent mechanism. *J. Cell Biol.* **2001**, *153* (6), 1175−1186.
(56) Tzima, E.; del Pozo, M. A.; Shattil, S. J.; Chien, S.; Schwartz, M. A. Activation of integrins in endothelial cells by fluid shear stress mediates Rho-dependent cytoskeletal alignment. *EMBO J.* **2001**, *20* (17), 4639−4647.
(57) Wang, N.; Butler, J. P.; Ingber, D. E. Mechanotransduction across the cell surface and through the cytoskeleton. *Science* **1993**, *260* (5111), 1124−1127.
(58) Choquet, D.; Felsenfeld, D. P.; Sheetz, M. P. Extracellular matrix rigidity causes strengthening of integrin-cytoskeleton linkages. *Cell* **1997**, *88* (1), 39−48.
(59) Khan, S.; Sheetz, M. P. Force effects on biochemical kinetics. *Annu. Rev. Biochem.* **1997**, *66*, 785−805.
(60) Ingber, D. E. Tensegrity: the architectural basis of cellular mechanotransduction. *Annu. Rev. Physiol.* **1997**, *59*, 575−599.
(61) Ingber, D. Integrins as mechanochemical transducers. *Curr. Opin. Cell Biol.* **1991**, *3* (5), 841−848.
(62) Zhong, C.; Chrzanowska-Wodnicka, M.; Brown, J.; Shaub, A.; Belkin, A. M.; Burridge, K. Rho-mediated contractility exposes a cryptic site in fibronectin and induces fibronectin matrix assembly. *J. Cell Biol.* **1998**, *141* (2), 539−551.
(63) Baneyx, G.; Baugh, L.; Vogel, V. Fibronectin extension and unfolding within cell matrix fibrils controlled by cytoskeletal tension. *Proc. Natl. Acad. Sci. U.S.A.* **2002**, *99* (8), 5139−5143.
(64) Sawada, Y.; Sheetz, M. P. Force transduction by Triton cytoskeletons. *J. Cell Biol.* **2002**, *156* (4), 609−615.
(65) Yoshigi, M.; Hoffman, L. M.; Jensen, C. C.; Yost, H. J.; Beckerle, M. C. Mechanical force mobilizes zyxin from focal adhesions to actin filaments and regulates cytoskeletal reinforcement. *J. Cell Biol.* **2005**, *171* (2), 209−215.
(66) Sawada, Y.; Nakamura, K.; Doi, K.; Takeda, K.; Tobiume, K.; Saitoh, M.; Morita, K.; Komuro, I.; De Vos, K.; Sheetz, M.; Ichijo, H. Rap1 is involved in cell stretching modulation of p38 but not ERK or JNK MAP kinase. *J. Cell Sci.* **2001**, *114* (Pt 6), 1221−1227.
(67) von Wichert, G.; Jiang, G.; Kostic, A.; De Vos, K.; Sap, J.; Sheetz, M. P. RPTP-alpha acts as a transducer of mechanical force on alphav/beta3-integrin-cytoskeleton linkages. *J. Cell Biol.* **2003**, *161* (1), 143−153.
(68) Kostic, A.; Sheetz, M. P. Fibronectin rigidity response through Fyn and p130Cas recruitment to the leading edge. *Mol. Biol. Cell* **2006**, *17* (6), 2684−2695.
(69) Bershadsky, A.; Kozlov, M.; Geiger, B. Adhesion-mediated mechanosensitivity: a time to experiment, and a time to theorize. *Curr. Opin. Cell Biol.* **2006**, *18* (5), 472−481.

Received April 11, 2007. Accepted July 11, 2007.

BP070110A